

Multiparameter quantum estimation under dephasing noise

Le Bin Ho,^{1,*} Hideaki Hakoshima,² Yuichiro Matsuzaki,² Masayuki Matsuzaki,³ and Yasushi Kondo^{1,4}

¹*Department of Physics, Kindai University, Higashi-Osaka, 577-8502, Japan*

²*Nanoelectronics Research Institute, National Institute of Advanced Industrial Science and Technology (AIST), Ibaraki 305-8568, Japan*

³*Department of Physics, Fukuoka University of Education, Munakata, Fukuoka 811-4192, Japan*

⁴*Interdisciplinary Graduate School of Science and Engineering, Kindai University, Higashi-Osaka, 577-8502, Japan*

(Dated: July 6, 2021)

Simultaneous quantum estimation of multiple parameters has recently become essential in quantum metrology. Although the ultimate sensitivity of a multiparameter quantum estimation in noiseless environments can beat the standard quantum limit that every classical sensor is bounded by, it is unclear whether the quantum sensor has an advantage over the classical one under realistic noise. In this work, we present a framework of the simultaneous estimation of multiple parameters with quantum sensors in a certain noisy environment. Our multiple parameters to be estimated are three components of an external magnetic field, and we consider the noise that causes only dephasing. We show that there is an optimal sensing time in the noisy environment and the sensitivity can beat the standard quantum limit when the noisy environment is non-Markovian.

I. INTRODUCTION

Quantum estimation theory is a mathematical framework behind quantum metrology and is important for scientific researches and technological applications. Some of its demanded tasks are minimizing the uncertainty of the estimation and attaining an ultimate bound imposed by fundamental laws of quantum mechanics.

Great efforts both in theoretical and experimental works have been devoted to single-parameter estimation [1–16]. One of the practical applications of the single parameter estimation is to measure external fields such as magnetic fields or electric fields. When the resonance of a solid-state qubit is shifted by external fields, we can use a superposition state of the qubit to estimate the amplitude of the external fields with a Ramsey type measurements. With the use of N individual qubits, we can decrease the uncertainty of the estimation by $\delta\phi = \mathcal{O}(N^{-\frac{1}{2}})$, which is called the standard quantum limit (SQL). (Here, ϕ is a single estimated parameter.) Moreover, by exploiting entanglement among N qubits, we can in principle obtain $\delta\phi = \mathcal{O}(N^{-1})$ in the ideal circumstance, and this scaling is called the Heisenberg limit (HL) [1, 5, 6].

However, since the entanglement is fragile against decoherence, it is not trivial whether the entanglement is useful to decrease the uncertainty of the estimation under the effect of realistic noise. The effect of noise in the cases of single-parameter estimations has been theoretically [2, 10, 17–24] and experimentally [7, 25–30] discussed. The most important noise for the solid-state qubits is the dephasing one. It is known that one cannot beat the SQL for the estimation of the field amplitude under the effect of Markovian dephasing noise even with the use of

the entanglement [2]. On the other hand, recent studies show that, if the dephasing noise has non-Markovian properties, one can obtain the scaling of $\delta\phi = \mathcal{O}(N^{-3/4})$ by using the entanglement for single parameter estimation, and this scaling beats the SQL [7, 18, 31–35]. The crucial feature of the non-Markovian noise is to show a quadratic behavior as a function of time at the initial decay, which is called a Zeno regime, and the interaction time between the entanglement and target fields is adjusted in this regime to obtain the quantum enhancement of the sensitivity [7, 18, 31–36]. For the estimation of the amplitude of the field, $\delta\phi = \mathcal{O}(N^{-3/4})$ is considered as the ultimate scaling under the effect of the non-Markovian dephasing noise [32, 34, 35].

On the other hand, great attention has been paid to multiparameter estimations [37, 38]. For example, estimations of phase and phase diffusion (loss) [39–46], phase-space displacements [47, 48], multiple phases [38, 49–51], damping and temperature [52], waveforms [53], and operators [54, 55]. One of the practical applications of the multiparameter estimation is to measure vector magnetic fields. Imaging of the vector magnetic fields from the biomaterials or circuit current is especially important for the medical and materials science, and these have been discussed and demonstrated [56, 57].

In this work, we numerically investigate the multiparameter estimation under the influence of dephasing noise. In particular, we consider the case to estimate three vector components of the target fields by using the entanglement under the effect of dephasing noise. Moreover, we study the performance of the entangled sensor for multiparameter estimation under both Markovian and non-Markovian dephasing noises. Although numerical calculations of noisy quantum systems with many qubits are difficult because the size of the density matrix grows exponentially as the number of the qubits increases, the recent studies show that the cost for the calculation is tractable when the qubits are identical two-

* Electronic address: binho@kindai.ac.jp

Current address: Research Institute of Electrical Communication, Tohoku University, Sendai 980-8577, Japan

level systems [58–60]. We adopt this technique, and numerically calculate the uncertainty of the estimation to check how the uncertainty scales as a function of the number of the qubits. We show that, under the effect of non-Markovian dephasing noise, we can beat the SQL for the multiparameter estimation, and the scaling that we obtain by fitting the numerical results $\delta\phi = \mathcal{O}(N^{-3/4})$, which is the same as that of the ultimate scaling for the single parameter estimation under dephasing noise. (Here, vector ϕ is a set of multiple parameters.) Our analysis would provide further understanding of quantum metrology.

This paper is organized as follows. Section II introduces our measurement framework estimating multiple parameters simultaneously. The numerical results are presented in Sec. III. We summarize our work in Sec. IV.

II. MULTIPARAMETER ESTIMATION FRAMEWORK

A. Dynamics of an N -identical particles sensor

We consider a sensor consisting of an ensemble of N -identical two-level systems. The two-level system at the n th site can be characterized by the Pauli operators as $J_\alpha^{(n)} = \frac{1}{2}\sigma_\alpha^{(n)}$ for $\alpha = \{x, y, z\}$. The whole sensor operators are given as $J_\alpha = \sum_n J_\alpha^{(n)}$. To be concrete, we assume that these two-level systems are one-half spins and that the field to be sensed is a magnetic field.

The sensor dynamics without noise is governed by the Hamiltonian

$$H(\phi) = \phi_x J_x + \phi_y J_y + \phi_z J_z, \quad (1)$$

where a set of three parameters $\phi = (\phi_x, \phi_y, \phi_z)$ describes the magnetic field to be estimated. Also, this magnetic field provides the quantization axis of each qubit. We assume the sensor is governed by the GKLS master equation [61],

$$\frac{d\rho_t(\phi)}{dt} = -i[H(\phi), \rho_t(\phi)] + \mathcal{L}[\rho_t(\phi)], \quad (2)$$

where $\rho_t(\phi)$ is the quantum state of the sensor at time t , and we take the natural unit system, or $\hbar = 1$. Further, we assume the followings

$$\mathcal{L}[\rho_t(\phi)] = -\gamma_t \sum_{n=1}^N [a^{(n)}, [a^{(n)}, \rho_t(\phi)]], \quad (3)$$

where γ_t characterizes the strength of the noise and

$$a^{(n)} = \boldsymbol{\varphi} \cdot \mathbf{J}^{(n)} = \varphi_x J_x^{(n)} + \varphi_y J_y^{(n)} + \varphi_z J_z^{(n)}, \quad (4)$$

where $a^{(n)}$ is the operator acting on the n th-site spin and is normalized so that $[a^{(n)}]^2 = \mathbf{I}$, or $\varphi_x^2 + \varphi_y^2 + \varphi_z^2 = 4$.

Then, we consider dephasing noise by assuming $\phi \parallel \boldsymbol{\varphi}$ where the environmental noisy fields are applied along

the quantization axis of the system. A similar noise has been considered in single parameter estimation in Refs. [18, 31, 37]. This assumption leads to the property such that $H(\phi)$ and $a^{(n)}$ commute and thus the sensor dynamics calculation becomes tractable. Such a dephasing noise is often considered as a dominant noise in the solid-state systems and NMR.

A Markovian and non-Markovian noisy environment can be introduced by taking the noise strength γ_t as

$$\gamma_t = \begin{cases} \gamma & : \text{Markovian} \\ \gamma^2 t & : \text{non-Markovian} \end{cases}. \quad (5)$$

We provide a detailed calculation for the dynamics of such a sensor in Appendices A and B.

B. The precision of the estimation

The precision of the estimation of ϕ is evaluated by its covariance matrix, $[\mathbf{V}(\phi)]_{\alpha,\beta} = \langle \phi_\alpha \phi_\beta \rangle - \langle \phi_\alpha \rangle \langle \phi_\beta \rangle$. The diagonal elements $[\mathbf{V}(\phi)]_{\alpha,\alpha}$ are the variance $(\delta\phi_\alpha)^2$ while the off-diagonal elements are the correlations between different parameters. The quantum Cramér-Rao bound is a lower bound to the covariance matrix in terms of the classical Fisher information matrix (CFIM) and quantum Fisher information matrix (QFIM), such that

$$M \cdot \mathbf{V}(\phi) \geq [\mathbf{F}(\phi)]^{-1} \geq [\mathbf{Q}(\phi)]^{-1}, \quad (6)$$

where M is the number of repeated measurements in the total measurement time T , \mathbf{F} and \mathbf{Q} are the CFIM and QFIM, respectively. The first inequality is a classical Cramér-Rao bound (CCRB), while the second one is referred to as a quantum Cramér-Rao bound (QCRB). The CFIM is given through the measurement probabilities $[\mathbf{F}(\phi)]_{\alpha\beta} = \sum_l \frac{1}{P(l|\phi)} [\partial_\alpha P(l|\phi)] [\partial_\beta P(l|\phi)]$, where $\{\alpha, \beta\} = \{x, y, z\}$ and $P(l|\phi) = \text{Tr}[\Pi_l \rho_t(\phi)]$ determined by a POVM $\{\Pi_l\}$ and where we have used $\partial_\alpha \rho_t(\phi) \equiv \frac{\partial \rho_t(\phi)}{\partial \phi_\alpha}$ for short. When $\rho_t(\phi)$ is able to be spectral decomposed so that $\rho_t(\phi) = \sum_l p_l |l\rangle\langle l|$, the QFIM is given by

$$[\mathbf{Q}(\phi)]_{\alpha,\beta} = 2 \sum_{p_l + p_{l'} > 0} \frac{\langle l | \partial_\alpha \rho_t(\phi) | l' \rangle \langle l' | \partial_\beta \rho_t(\phi) | l \rangle}{p_l + p_{l'}}. \quad (7)$$

Although the number of l is exponentially large (2^N), we can reduce the calculation cost of which order is N^2 when the qubits are symmetric in terms of permutation operations (See Appendix A for details).

From the trace of Eq. (6), we will analyze the lower bound of the total variance

$$|\delta\phi|^2 \geq \text{Tr}[[\mathbf{Q}(\phi)]^{-1}]/M, \quad (8)$$

where $|\delta\phi|^2 \equiv \text{Tr}[\mathbf{V}(\phi)]$ is the total variance, which is the summation of three partial variances, i.e., $|\delta\phi|^2 = |\delta\phi_x|^2 + |\delta\phi_y|^2 + |\delta\phi_z|^2$. The lower bound in the R.H.S. of Eq. (8) is the ultimate bound that all three components can be achieved simultaneously.

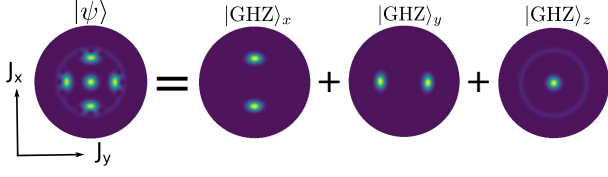


FIG. 1. (Color online) The visualization of Husimi functions for $|\text{GHZ}\rangle_k$, ($k = x, y, z$) and $|\psi\rangle$ given in Eq. (9). We fixed $N = 40$.

III. NUMERICAL RESULTS

A. Simultaneous versus individual scenarios

We consider two scenarios for the estimation: simultaneous estimation and individual estimation. For the simultaneous scenario, three components of the field will be estimated simultaneously. The initial state is set to be $\rho_{t=0} = |\psi\rangle\langle\psi|$, where

$$|\psi\rangle = \mathcal{N}(|\text{GHZ}\rangle_x + |\text{GHZ}\rangle_y + |\text{GHZ}\rangle_z), \quad (9)$$

\mathcal{N} is the normalization constant. The GHZ state is defined as

$$|\text{GHZ}\rangle_k = \frac{|\lambda_k^{\max}\rangle + |\lambda_k^{\min}\rangle}{\sqrt{2}}, \quad (10)$$

where $|\lambda_k^{\max}\rangle$ and $|\lambda_k^{\min}\rangle$ are the two eigenstates of J_k ($k = x, y, z$) that correspond to the maximum and minimum eigenvalues λ_k^{\max} and λ_k^{\min} , respectively. If there is no noise, an entanglement sensor using the state $|\psi\rangle$ provides the Heisenberg scaling for the multiparameter estimation as shown in Ref. [38]. In Fig. 1, we visualize the Husimi function [62] of the three GHZ states and $|\psi\rangle$ for $N = 40$.

For the individual scenario, each component will be estimated separately after repeated $M/3$ measurements. In this case, we use an entangled state $|\text{GHZ}\rangle_k$ in Eq. (10) ($k = x, y, z$) to measure the corresponding magnetic field. This scheme is a direct application of the single parameter estimation to the vector field sensing.

We define the lower bound of the total variance in Eq. (8) for the simultaneous scenario as

$$\mathcal{I}_{\text{sim}} \equiv \text{Tr}[\mathbf{Q}(\phi)]^{-1}/M, \quad (11)$$

where ‘sim’ stands for ‘simultaneous.’ Although the use of such a lower bound may not provide full insight into the variance, we emphasize that such a lower bound can be in principle achieved by using an optimal minimization scheme such as SDP [37] or a general JNT-QEC [63].

For the individual scenario, we define the total variance as

$$\mathcal{I}_{\text{ind}} = \frac{3}{M} \left(Q_x^{-1} + Q_y^{-1} + Q_z^{-1} \right), \quad (12)$$

where $Q_k = [\mathbf{Q}(\phi)]_{k,k}$ ($k = x, y, z$) setting the initial state $|\text{GHZ}\rangle_k$. Here, $\frac{3}{M}$ denotes $M/3$ repeated measurements devoted to estimating a component k .

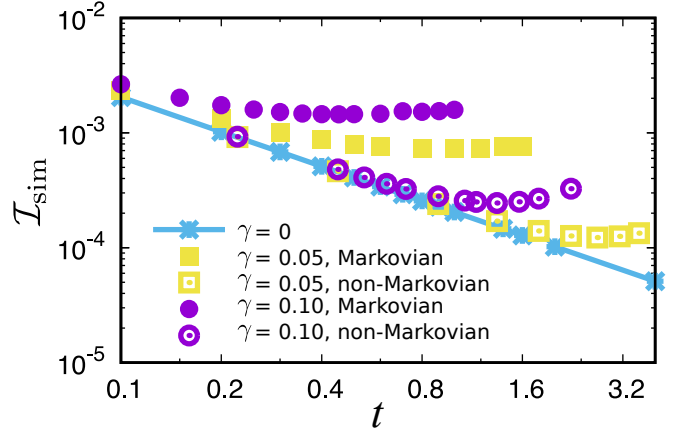


FIG. 2. (Color online) The plot of $\mathcal{I}_{\text{sim}} \equiv \text{Tr}[\mathbf{Q}(\phi)]^{-1}/M$ as a function of measurement time t at $T = 100$ and $N = 20$ at $\gamma = 0.1$ and 0.05 in both Markovian and non-Markovian dephasing noisy environment. \mathcal{I}_{sim} 's at $\gamma = 0$ are plotted for comparison. Note that $M = T/t$.

We emphasize that our framework here is different from Ref. [38]. While Ref. [38] studies the noiseless case, here we have extended its calculation technique for a sensor under noise.

B. The total variance under the dephasing noise

Here, we investigate the performance of the entangled sensor for the multiparameter estimation under the effect of the dephasing noise. To examine the numerical results, we fix $\varphi = (2/\sqrt{3}, 2/\sqrt{3}, 2/\sqrt{3})$ in Eq. (4) and $\phi = (0.01, 0.01, 0.01)$ in Eq. (1). Here, we assume, as usual, that the necessary time for the state preparation and readout is negligibly small. We fix the total time $T = 100$ and investigate \mathcal{I} for Markovian and non-Markovian cases.

Figure 2 shows \mathcal{I}_{sim} as a function of measurement time t for $N = 20$. Note that we are allowed to measure for T and thus $M = T/t$ in Eq. (11). We investigate $\gamma = 0, 0.05$, and 0.1 cases. In the absence of noise ($\gamma = 0$), the longer t always gives the better measurements. When the noise is present ($\gamma \neq 0$), we found that there are minima of \mathcal{I}_{sim} as a function of t : There are optimal measurement times t^{opt} 's as functions of N . t^{opt} in the case of Markovian noise is shorter than that in the case of non-Markovian one.

We investigate t^{opt} as a function of N for both simultaneous ($\circ = \text{sim}$) and individual ($\circ = \text{ind}$) scenarios in both Markovian and non-Markovian cases. Figure 3 shows that $1/t^{\text{opt}}$ is proportional to N (\sqrt{N}) in the Markovian (non-Markovian) case at $N \geq 10$, as expected [2, 31]. We found, however, that t^{opt} 's behave differently at $N < 10$ in both Markovian and non-Markovian cases. We suspect that $N < 10$ is too small to observe the expected dependences. These observations are consistent

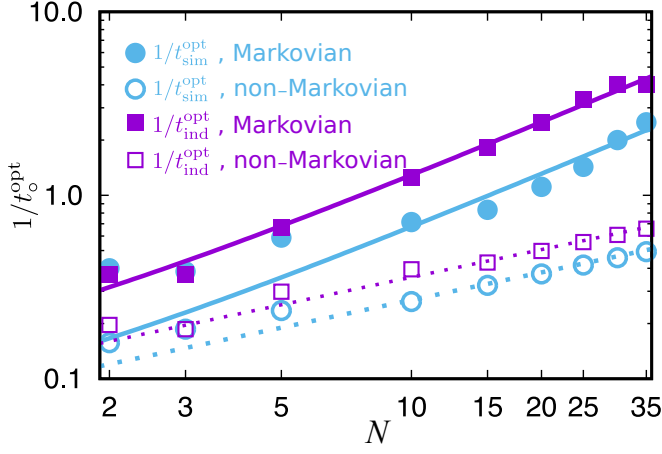


FIG. 3. (Color online) $1/t_{\circ}^{\text{opt}}$ as a function of N for two cases of Markovian and non-Markovian dephasing noisy environments. Here $\circ = \text{sim}$ or ind . The dotted lines show \sqrt{N} dependence, while the solid lines do N dependence. We fit the data for $N \geq 10$.

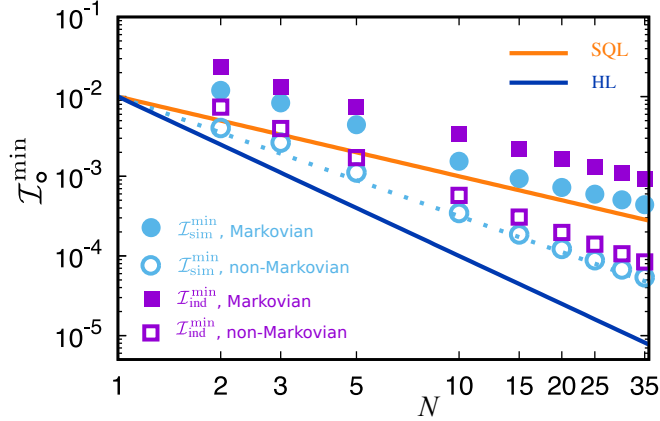


FIG. 4. (Color online) $\mathcal{I}_{\circ}^{\min}$ as a function of N in the Markovian and non-Markovian dephasing noisy environments when $\gamma = 0.05$. To show the SQL and HL dependences, $1/TN$ (orange line, SQL) and $1/TN^2$ (blue line, HL) are plotted. The line $1/TN^{1.5}$ is also plotted (cyan dotted line).

with N dependences of $\mathcal{I}_{\circ}^{\min}$ in Fig. 4.

Figure 4 shows $\mathcal{I}_{\circ}^{\min}$ for $\gamma = 0.05$ at $t = t_{\circ}^{\text{opt}}$, as a function of N . Here $\circ = \text{sim}$ or ind . We observe the followings for the Markovian case. (i) $\mathcal{I}_{\circ}^{\min}$ becomes proportional to N^{-1} at $N \geq 10$ or has the same dependence with the SQL and thus the entangled sensor has no benefit, and (ii) $\mathcal{I}_{\text{ind}}^{\min} > \mathcal{I}_{\text{sim}}^{\min}$ at the same N which implies that the

simultaneous measurement is beneficial. Those behaviors are consistent with the case of the single parameter estimation where entangled sensors cannot beat the SQL under the effect of the Markovian dephasing noise [2].

In contrast, we observe the followings for the non-Markovian case. (i) $\mathcal{I}_{\circ}^{\min}$ is proportional to $N^{-1.5}$ at $N \geq 10$ and thus the entangled sensor is beneficial, and (ii) $\mathcal{I}_{\text{ind}}^{\min} > \mathcal{I}_{\text{sim}}^{\min}$ (although this difference is small) at the same N which implies that the simultaneous measurement is beneficial. The observation (i) ($N^{-1.5}$ dependence) is a well-known scaling for non-Markovian dephasing [18, 31]. The observation (ii) was reported in Ref. [38] for a noiseless case. Whereas, in this work, we show the reduction of uncertainty in noisy cases.

IV. CONCLUSION

In conclusion, we analyze the simultaneous estimation of the multiple parameters with an entangled sensor in both Markovian and non-Markovian dephasing noisy environment. We found that the entangled sensor is beneficial in the non-Markovian environment while it is not the case in the Markovian one.

Our multiple parameters are the components of a magnetic field and are sensed with an ensemble of N -identical particles that are entangled with each other. By taking into account the symmetry in permutation operators, the calculation cost is drastically reduced and becomes tractable. The entangled sensor is exposed to the target fields under the effect of the dephasing noise. We numerically calculate the quantum Fisher information matrix and investigate the lower bound of the total variance, denoted as \mathcal{I} . When the dephasing noise is present, it always prevents us from achieving the Heisenberg limit. We, however, found that an entangled sensor can beat the standard quantum limit in a non-Markovian dephasing noise but not in a Markovian noise.

ACKNOWLEDGMENTS

This work was supported by CREST(JPMJCR1774), JST. This work was also supported by Leading Initiative for Excellent Young Researchers MEXT Japan, MEXT KAKENHI (Grant No. 15H05870), and JST presto (Grant No. JPMJPR1919) Japan. LBH is grateful to Nathan Shammah for useful discussions on QuTiP.

Appendix A: Permutation symmetric sensor

We consider the sensor consists of N -identical particles where the permutation symmetry is taken as follows [60, 64, 65]. The joint Hilbert space of the sensor is $\mathcal{H}_N = \mathcal{H}^{(1)} \otimes \cdots \otimes \mathcal{H}^{(N)}$ with $\dim(\mathcal{H}_N) = 2^N$. Any quantum state

of the sensor can be given as

$$|\psi\rangle = \sum_{m_1, m_2, \dots, m_N} c_{m_1, m_2, \dots, m_N} |m_1, m_2, \dots, m_N\rangle, \quad (\text{A.1})$$

where the product basis $|m_1, m_2, \dots, m_N\rangle = |m_1\rangle \otimes |m_2\rangle \otimes \dots \otimes |m_N\rangle$, with $m_n = \pm \frac{1}{2}$ are eigenvalues of $J_z^{(n)}$. This basis is the eigenstate of the spin operators $\mathbf{J}^{(n)}$ and $J_z^{(n)}$

$$[\mathbf{J}^{(n)}]^2 |m_1, m_2, \dots, m_N\rangle = j_n(j_n + 1) |m_1, m_2, \dots, m_N\rangle, \quad (\text{A.2})$$

$$J_z^{(n)} |m_1, m_2, \dots, m_N\rangle = m_n |m_1, m_2, \dots, m_N\rangle. \quad (\text{A.3})$$

The above product basis can be represented by an irrep basis, which consists of the total spin eigenstates [64, 65]

$$\mathbf{J}^2 |j, m, i\rangle = j(j+1) |j, m, i\rangle, \quad (\text{A.4})$$

$$J_z |j, m, i\rangle = m |j, m, i\rangle, \quad (\text{A.5})$$

where $|j, m, i\rangle$ is the irrep basis, $j \leq N/2$ the total angular momentum, $|m| \leq j$. For each j , the quantum number $i = 1, \dots, d_N^j$, where

$$d_N^j = \frac{N!(2j+1)}{(N/2-j)!(N/2+j+1)!} \quad (\text{A.6})$$

is the number of degenerate irreps for each j [66] (the number of ways to combine N particles that gets the total angular momentum j .) The coefficient c_{m_1, m_2, \dots, m_N} now becomes $c_{j, m, i}$. Taking into account the permutation symmetry where all the degenerate irreps of each j are indistinguishable, i.e., $c_{j, m, i} = c_{j, m, i'} \forall i, i' \in [1, d_N^j]$, then, the irrep basis $|j, m, i\rangle$ can be gathered to the Dicke basis $|j, m\rangle$ [67], where

$$|j, m\rangle = \frac{1}{\sqrt{d_N^j}} \sum_{i=1}^{d_N^j} |j, m, i\rangle. \quad (\text{A.7})$$

This basis is the eigenstate of the collective pseudo-spin operators

$$\mathbf{J}^2 |j, m\rangle = j(j+1) |j, m\rangle, \quad (\text{A.8})$$

$$J_z |j, m\rangle = m |j, m\rangle. \quad (\text{A.9})$$

Under this symmetry, the dimension now reduces to the Dicke-basis dimension d_D :

$$d_D = \begin{cases} (N+3)(N+1)/4 & \text{for odd } N, \\ (N+2)^2/4 & \text{for even } N. \end{cases} \quad (\text{A.10})$$

Hereafter, we take \mathbf{J}, J_α as the collective pseudo-spin operators in the d_D dimension.

In the d_D dimension, J_α has a structure of block matrices as shown in Fig. 5. The first block corresponds to $j = N/2$, the explicit form of this block is a spin- j operator $S_\alpha, \alpha = \{x, y, z\}$. The construction for others is the same. For example, $N = 3$, we have

$$J_x = \begin{pmatrix} 0 & \sqrt{3}/2 & 0 & 0 & 0 & 0 \\ \sqrt{3}/2 & 0 & 2 & 0 & 0 & 0 \\ 0 & 2 & 0 & \sqrt{3}/2 & 0 & 0 \\ 0 & 0 & \sqrt{3}/2 & 0 & 0 & 0 \\ 0 & 0 & 0 & 0 & 0 & 1/2 \\ 0 & 0 & 0 & 0 & 1/2 & 0 \end{pmatrix}. \quad (\text{A.11})$$

Do the same for J_y and J_z .

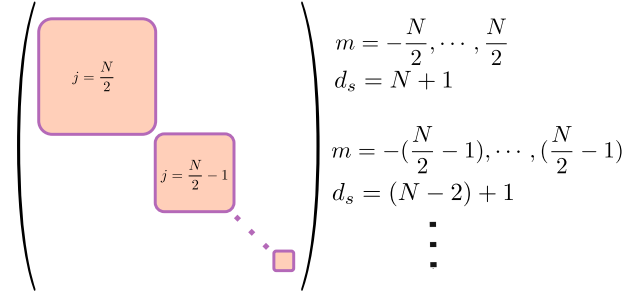


FIG. 5. (Color online) Block-diagonal form of a quantum state representing in the Dicke basis. The first block corresponds to $j = N/2$ and its sub-dimension is $d_s = N + 1$. Do the same calculation for the remaining blocks in the diagonal matrix. The off-diagonal terms are all zeros.

Appendix B: Dynamic of permutation symmetric sensor under dephasing noise

We will solve the GKLS equation (2) in the main text in d_D dimension. We note that $[H(\phi), a^{(n)}] = 0$, thus, we first calculate only the Liouville term (3). The following expressions are independent of the choice of the direction of the quantization axis, which is physically determined by the target field to be measured. We rewrite it here:

$$\frac{\partial \rho_t}{\partial t} = 2\gamma_t \left(\sum_{n=1}^N a^{(n)} \rho_t a^{(n)} - N \rho_t \right). \quad (\text{B.1})$$

We first show how to calculate the Liouvillian superoperator in the R.H.S. of Eq. (B.1). Using $a^{(n)} = \varphi_x J_x^{(n)} + \varphi_y J_y^{(n)} + \varphi_z J_z^{(n)}$, the summation term in Eq. (B.1) is: (for short, we first keep ρ_t)

$$\begin{aligned} \sum_{n=1}^N a^{(n)} \rho_t a^{(n)} &= \sum_{n=1}^N \left[\varphi_x J_x^{(n)} + \varphi_y J_y^{(n)} + \varphi_z J_z^{(n)} \right] \rho_t \left[\varphi_x J_x^{(n)} + \varphi_y J_y^{(n)} + \varphi_z J_z^{(n)} \right] \\ &= \sum_{n=1}^N \left[\frac{\varphi_x}{2} (J_+^{(n)} + J_-^{(n)}) + \frac{i\varphi_y}{2} (J_-^{(n)} - J_+^{(n)}) + \varphi_z J_z^{(n)} \right] \rho_t [\dots] \\ &= \sum_{n=1}^N \left[\varphi_w^* J_+^{(n)} + \varphi_w J_-^{(n)} + \varphi_z J_z^{(n)} \right] \rho_t \left[\varphi_w^* J_+^{(n)} + \varphi_w J_-^{(n)} + \varphi_z J_z^{(n)} \right], \end{aligned} \quad (\text{B.2})$$

where $J_{\pm}^{(n)} = J_x^{(n)} \pm iJ_y^{(n)}$, $\varphi_w = (\varphi_x + i\varphi_y)/2$. Finally, we have

$$\begin{aligned} \sum_{n=1}^N a^{(n)} \rho_t a^{(n)} &= \sum_{n=1}^N \left[(\varphi_w^*)^2 J_+^{(n)} \rho_t J_+^{(n)} + |\varphi_w|^2 J_+^{(n)} \rho_t J_-^{(n)} + \varphi_w^* \varphi_z J_+^{(n)} \rho_t J_z^{(n)} \right. \\ &\quad + |\varphi_w|^2 J_-^{(n)} \rho_t J_+^{(n)} + (\varphi_w)^2 J_-^{(n)} \rho_t J_-^{(n)} + \varphi_w \varphi_z J_-^{(n)} \rho_t J_z^{(n)} \\ &\quad \left. + \varphi_w^* \varphi_z J_z^{(n)} \rho_t J_+^{(n)} + \varphi_w \varphi_z J_z^{(n)} \rho_t J_-^{(n)} + \varphi_z^2 J_z^{(n)} \rho_t J_z^{(n)} \right]. \end{aligned} \quad (\text{B.3})$$

Here, these terms corresponding to $J_+^{(n)} \rho_t J_-^{(n)}$, $J_-^{(n)} \rho_t J_+^{(n)}$, and $J_z^{(n)} \rho_t J_z^{(n)}$ are local pumping, local emission, and local dephasing, respectively. Now, using $\rho_t = \sum_{jmm'} p_{jmm'} |j, m\rangle \langle j, m'|$. Then for each j, m, m' , we have [60, 64, 65]

$$\begin{aligned} \sum_{n=1}^N J_k^{(n)} |j, m\rangle \langle j, m'| J_l^{(n)\dagger} &= a_{kl}^N |j, m_k\rangle \langle j, m'_l| \\ &\quad + b_{kl}^N |j-1, m_k\rangle \langle j-1, m'_l| \\ &\quad + d_{kl}^N |j+1, m_k\rangle \langle j+1, m'_l|, \end{aligned} \quad (\text{B.4})$$

where $k, l = \{+, -, z\}$, $m_+ = m + 1$, $m_- = m - 1$, $m_z = m$, and

$$\begin{aligned} a_{kl}^N &= A_k^{j,m} A_l^{j,m'} \frac{1}{2j} \left(1 + \frac{\alpha_N^{j+1}}{d_N^j} \frac{2j+1}{j+1} \right), \\ &= A_k^{j,m} A_l^{j,m'} \frac{N/2+1}{2j(j+1)} \\ &:= A_k^{j,m} A_l^{j,m'} \Lambda_a, \end{aligned} \quad (\text{B.5})$$

$$\begin{aligned} b_{kl}^N &= B_k^{j,m} B_l^{j,m'} \frac{\alpha_N^j}{2j d_N^j}, \\ &= B_k^{j,m} B_l^{j,m'} \frac{N/2+j+1}{2j(2j+1)} \\ &:= B_k^{j,m} B_l^{j,m'} \Lambda_b, \end{aligned} \quad (\text{B.6})$$

$$\begin{aligned} d_{kl}^N &= D_k^{j,m} D_l^{j,m'} \frac{\alpha_N^{j+1}}{2(j+1)d_N^j}, \\ &= D_k^{j,m} D_l^{j,m'} \frac{N/2-j}{2(j+1)(2j+1)} \\ &:= D_k^{j,m} D_l^{j,m'} \Lambda_d, \end{aligned} \quad (\text{B.7})$$

where

$$A_{\pm}^{j,m} = \sqrt{(j \mp m)(j \pm m + 1)}, \quad A_z^{j,m} = m, \quad (\text{B.8})$$

$$B_{\pm}^{j,m} = \pm \sqrt{(j \mp m)(j \mp m - 1)}, \quad B_z^{j,m} = \sqrt{(j+m)(j-m)}, \quad (\text{B.9})$$

$$D_{\pm}^{j,m} = \mp \sqrt{(j \pm m + 1)(j \pm m + 2)}, \quad D_z^{j,m} = \sqrt{(j+m+1)(j-m+1)}, \quad (\text{B.10})$$

$$\Lambda_a = \frac{N/2+1}{2j(j+1)}, \quad \Lambda_b = \frac{N/2+j+1}{2j(2j+1)}, \quad \Lambda_d = \frac{N/2-j}{2(j+1)(2j+1)}, \quad (\text{B.11})$$

and

$$\alpha_N^j = \sum_{j'=j}^{N/2} d_N^{j'} = \frac{N!}{(N/2-j)!(N/2+j)!}, \quad (\text{B.12})$$

with the degenerate $d_N^j = \frac{N!(2j+1)}{(N/2-j)!(N/2+j+1)!}$.

We calculate explicitly Eq. (B.4) for each j, m, m' , where

$$\begin{aligned} \varphi_z^2 \sum_{n=1}^N J_z^{(n)} |j, m\rangle \langle j, m' | J_z^{(n)} &= \varphi_z^2 (m m' \Lambda_a |j, m\rangle \langle j, m'| \quad \leftarrow \Gamma^{(1)} \\ &+ B_z^{j,m} B_z^{j,m'} \Lambda_b |j-1, m\rangle \langle j-1, m'| \quad \leftarrow \Gamma^{(5)} \\ &+ D_z^{j,m} D_z^{j,m'} \Lambda_d |j+1, m\rangle \langle j+1, m'|) \quad \leftarrow \Gamma^{(6)} \end{aligned}$$

(the coefficients related to the term $|j, m\rangle \langle j, m'|$ will be assigned (\leftarrow) to $\Gamma^{(1)}$ and so on.)

$$\begin{aligned} |\varphi_w|^2 \sum_{n=1}^N J_-^{(n)} |j, m\rangle \langle j, m' | J_+^{(n)} &= |\varphi_w|^2 (A_-^{j,m} A_-^{j,m'} \Lambda_a |j, m-1\rangle \langle j, m'-1| \quad \leftarrow \Gamma^{(2)} \\ &+ B_-^{j,m} B_-^{j,m'} \Lambda_b |j-1, m-1\rangle \langle j-1, m'-1| \quad \leftarrow \Gamma^{(3)} \\ &+ D_-^{j,m} D_-^{j,m'} \Lambda_d |j+1, m-1\rangle \langle j+1, m'-1|) \quad \leftarrow \Gamma^{(4)} \end{aligned}$$

$$|\varphi_w|^2 \sum_{n=1}^N J_+^{(n)} |j, m\rangle \langle j, m' | J_-^{(n)} = |\varphi_w|^2 (A_+^{j,m} A_+^{j,m'} \Lambda_a |j, m+1\rangle \langle j, m'+1| \quad \leftarrow \Gamma^{(8)}$$

$$+ B_+^{j,m} B_+^{j,m'} \Lambda_b |j-1, m+1\rangle \langle j-1, m'+1| \quad \leftarrow \Gamma^{(7)}$$

$$+ D_+^{j,m} D_+^{j,m'} \Lambda_d |j+1, m+1\rangle \langle j+1, m'+1|) \quad \leftarrow \Gamma^{(9)}$$

(note that $J_-^{(n)}$ becomes $J_+^{(n)\dagger}$ as in Eq. (B.4))

$$(\varphi_w^*)^2 \sum_{n=1}^N J_+^{(n)} |j, m\rangle \langle j, m' | J_+^{(n)} = (\varphi_w^*)^2 (A_+^{j,m} A_-^{j,m'} \Lambda_a |j, m+1\rangle \langle j, m'-1| \quad \leftarrow \Gamma^{(10)}$$

$$+ B_+^{j,m} B_-^{j,m'} \Lambda_b |j-1, m+1\rangle \langle j-1, m'-1| \quad \leftarrow \Gamma^{(11)}$$

$$+ D_+^{j,m} D_-^{j,m'} \Lambda_d |j+1, m+1\rangle \langle j+1, m'-1|) \quad \leftarrow \Gamma^{(12)}$$

$$\varphi_w^* \varphi_z \sum_{n=1}^N J_+^{(n)} |j, m\rangle \langle j, m' | J_z^{(n)} = \varphi_w^* \varphi_z (A_+^{j,m} m' \Lambda_a |j, m+1\rangle \langle j, m'| \quad \leftarrow \Gamma^{(13)}$$

$$+ B_+^{j,m} B_z^{j,m'} \Lambda_b |j-1, m+1\rangle \langle j-1, m'| \quad \leftarrow \Gamma^{(14)}$$

$$+ D_+^{j,m} D_z^{j,m'} \Lambda_d |j+1, m+1\rangle \langle j+1, m'|) \quad \leftarrow \Gamma^{(15)}$$

$$\varphi_w^2 \sum_{n=1}^N J_-^{(n)} |j, m\rangle \langle j, m' | J_-^{(n)} = \varphi_w^2 (A_-^{j,m} A_+^{j,m'} \Lambda_a |j, m-1\rangle \langle j, m'+1| \quad \leftarrow \Gamma^{(16)}$$

$$+ B_-^{j,m} B_+^{j,m'} \Lambda_b |j-1, m-1\rangle \langle j-1, m'+1| \quad \leftarrow \Gamma^{(17)}$$

$$+ D_-^{j,m} D_+^{j,m'} \Lambda_d |j+1, m-1\rangle \langle j+1, m'+1|) \quad \leftarrow \Gamma^{(18)}$$

$$\varphi_w \varphi_z \sum_{n=1}^N J_-^{(n)} |j, m\rangle \langle j, m' | J_z^{(n)} = \varphi_w \varphi_z (A_-^{j,m} m' \Lambda_a |j, m-1\rangle \langle j, m'| \quad \leftarrow \Gamma^{(19)}$$

$$+ B_-^{j,m} B_z^{j,m'} \Lambda_b |j-1, m-1\rangle \langle j-1, m'| \quad \leftarrow \Gamma^{(20)}$$

$$+ D_-^{j,m} D_z^{j,m'} \Lambda_d |j+1, m-1\rangle \langle j+1, m'|) \quad \leftarrow \Gamma^{(21)}$$

$$\varphi_w^* \varphi_z \sum_{n=1}^N J_z^{(n)} |j, m\rangle \langle j, m' | J_+^{(n)} = \varphi_w^* \varphi_z (m A_-^{j,m} \Lambda_a |j, m\rangle \langle j, m'-1| \quad \leftarrow \Gamma^{(22)}$$

$$+ B_z^{j,m} B_-^{j,m'} \Lambda_b |j-1, m\rangle \langle j-1, m'-1| \quad \leftarrow \Gamma^{(23)}$$

$$+ D_z^{j,m} D_-^{j,m'} \Lambda_d |j+1, m\rangle \langle j+1, m'-1|) \quad \leftarrow \Gamma^{(24)}$$

$$\varphi_w \varphi_z \sum_{n=1}^N J_z^{(n)} |j, m\rangle \langle j, m' | J_-^{(n)} = \varphi_w \varphi_z (m A_+^{j,m} \Lambda_a |j, m\rangle \langle j, m'+1| \quad \leftarrow \Gamma^{(25)}$$

$$+ B_z^{j,m} B_+^{j,m'} \Lambda_b |j-1, m\rangle \langle j-1, m'+1| \quad \leftarrow \Gamma^{(26)}$$

$$+ D_z^{j,m} D_+^{j,m'} \Lambda_d |j+1, m\rangle \langle j+1, m'+1|) \quad \leftarrow \Gamma^{(27)}$$

We collect all coefficients correspond to each $|\cdot, \cdot\rangle \langle \cdot, \cdot|$ and assign as $\Gamma^{(i)}$, where $i = 1, \dots, 27$ as following:

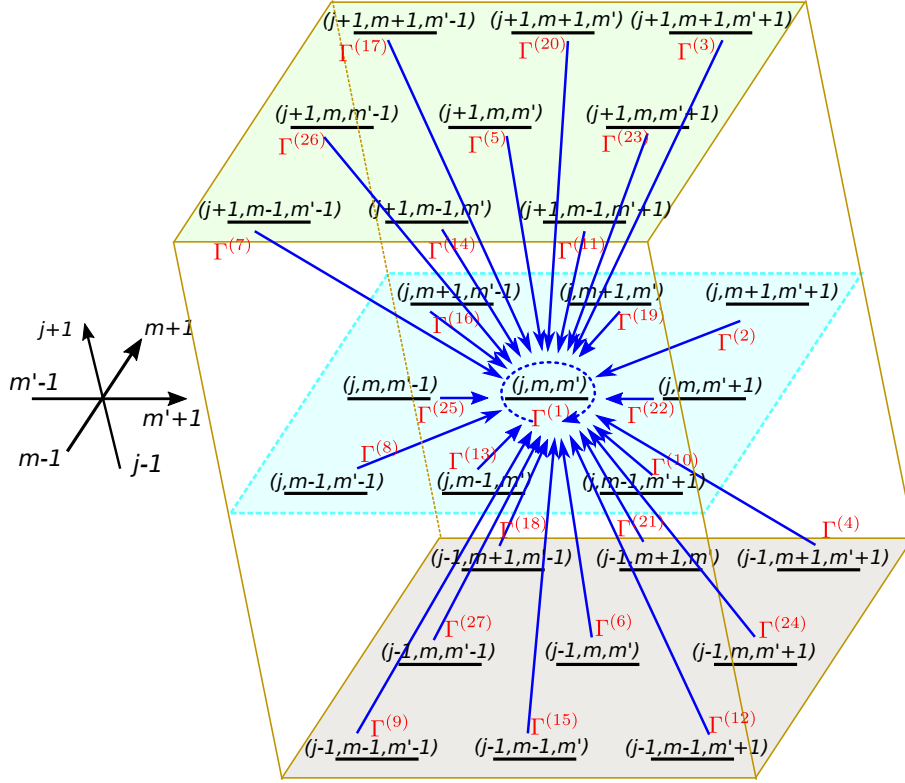


FIG. 6. (Color online) Sketch of the dynamics coupling given by a Dicke state, represented in terms of the coefficients $\Gamma^{(i)}$. We show the action of each coefficient onto a given Dicke state. All processes contribute to the coefficient $\Gamma^{(1)}$.

$m \backslash m'$	$\langle j-1, m'-1 $	$\langle j-1, m' $	$\langle j-1, m'+1 $	$\langle j, m'-1 $	$\langle j, m' $	$\langle j, m'+1 $	$\langle j+1, m'-1 $	$\langle j+1, m' $	$\langle j+1, m'+1 $
$ j-1, m-1\rangle$	$\Gamma^{(3)}$	$\Gamma^{(20)}$	$\Gamma^{(17)}$						
$ j-1, m\rangle$	$\Gamma^{(23)}$	$\Gamma^{(5)}$	$\Gamma^{(26)}$						
$ j-1, m+1\rangle$	$\Gamma^{(11)}$	$\Gamma^{(14)}$	$\Gamma^{(7)}$						
$ j, m-1\rangle$				$\Gamma^{(2)}$	$\Gamma^{(19)}$	$\Gamma^{(16)}$			
$ j, m\rangle$				$\Gamma^{(22)}$	$\Gamma^{(1)}$	$\Gamma^{(25)}$			
$ j, m+1\rangle$				$\Gamma^{(10)}$	$\Gamma^{(13)}$	$\Gamma^{(8)}$			
$ j+1, m-1\rangle$							$\Gamma^{(4)}$	$\Gamma^{(21)}$	$\Gamma^{(18)}$
$ j+1, m\rangle$							$\Gamma^{(24)}$	$\Gamma^{(6)}$	$\Gamma^{(27)}$
$ j+1, m+1\rangle$							$\Gamma^{(12)}$	$\Gamma^{(15)}$	$\Gamma^{(9)}$

Explicitly, we have

$$\begin{aligned}
 \Gamma^{(1)} &= 2\gamma_t(\varphi_z^2 m m' \Lambda_a - N) & \Gamma^{(10)} &= 2\gamma_t(\varphi_w^*)^2 A_+^{j,m} A_-^{j,m'} \Lambda_a & \Gamma^{(19)} &= 2\gamma_t \varphi_w \varphi_z A_-^{j,m} m' \Lambda_a \\
 \Gamma^{(2)} &= 2\gamma_t |\varphi_w|^2 A_-^{j,m} A_-^{j,m'} \Lambda_a & \Gamma^{(11)} &= 2\gamma_t(\varphi_w^*)^2 B_+^{j,m} B_-^{j,m'} \Lambda_b & \Gamma^{(20)} &= 2\gamma_t \varphi_w \varphi_z B_-^{j,m} B_-^{j,m'} \Lambda_b \\
 \Gamma^{(3)} &= 2\gamma_t |\varphi_w|^2 B_-^{j,m} B_-^{j,m'} \Lambda_b & \Gamma^{(12)} &= 2\gamma_t(\varphi_w^*)^2 D_+^{j,m} D_-^{j,m'} \Lambda_d & \Gamma^{(21)} &= 2\gamma_t \varphi_w \varphi_z D_-^{j,m} D_-^{j,m'} \Lambda_d \\
 \Gamma^{(4)} &= 2\gamma_t |\varphi_w|^2 D_-^{j,m} D_-^{j,m'} \Lambda_d & \Gamma^{(13)} &= 2\gamma_t \varphi_w^* \varphi_z A_+^{j,m} m' \Lambda_a & \Gamma^{(22)} &= 2\gamma_t \varphi_w^* \varphi_z m A_-^{j,m'} \Lambda_a \\
 \Gamma^{(5)} &= 2\gamma_t \varphi_z^2 B_z^{j,m} B_z^{j,m'} \Lambda_b & \Gamma^{(14)} &= 2\gamma_t \varphi_w^* \varphi_z B_+^{j,m} B_z^{j,m'} \Lambda_b & \Gamma^{(23)} &= 2\gamma_t \varphi_w^* \varphi_z B_z^{j,m} B_-^{j,m'} \Lambda_b \\
 \Gamma^{(6)} &= 2\gamma_t \varphi_z^2 D_z^{j,m} D_z^{j,m'} \Lambda_d & \Gamma^{(15)} &= 2\gamma_t \varphi_w^* \varphi_z D_+^{j,m} D_z^{j,m'} \Lambda_d & \Gamma^{(24)} &= 2\gamma_t \varphi_w^* \varphi_z D_z^{j,m} D_-^{j,m'} \Lambda_d \\
 \Gamma^{(7)} &= 2\gamma_t |\varphi_w|^2 B_+^{j,m} B_+^{j,m'} \Lambda_b & \Gamma^{(16)} &= 2\gamma_t \varphi_w^2 A_+^{j,m} A_+^{j,m'} \Lambda_a & \Gamma^{(25)} &= 2\gamma_t \varphi_w \varphi_z m A_+^{j,m'} \Lambda_a \\
 \Gamma^{(8)} &= 2\gamma_t |\varphi_w|^2 A_+^{j,m} A_+^{j,m'} \Lambda_a & \Gamma^{(17)} &= 2\gamma_t \varphi_w^2 B_-^{j,m} B_+^{j,m'} \Lambda_b & \Gamma^{(26)} &= 2\gamma_t \varphi_w \varphi_z B_z^{j,m} B_+^{j,m'} \Lambda_b \\
 \Gamma^{(9)} &= 2\gamma_t |\varphi_w|^2 D_+^{j,m} D_+^{j,m'} \Lambda_d & \Gamma^{(18)} &= 2\gamma_t \varphi_w^2 D_-^{j,m} D_+^{j,m'} \Lambda_d & \Gamma^{(27)} &= 2\gamma_t \varphi_w \varphi_z D_z^{j,m} D_+^{j,m'} \Lambda_d
 \end{aligned}$$

thus the equation can be solved. In the numerical calculation, we have extended the Permutational-Invariant Quantum Solver (PIQS) library in Qutip [60] using our analysis in this appendix.

Finally, $\rho_t(\phi)$ is given by the evolution $U(\phi)\rho_t U^\dagger(\phi)$.

Appendix C: Concrete calculation of the QFIM

For concreteness, to calculate the QFIM, we first derive the term $\partial\rho_t(\phi)/\partial\phi_k$ as

$$\begin{aligned}\partial_k\rho_t(\phi) &= \partial_k[U(\phi)\rho_tU^\dagger(\phi)] \\ &= \partial_kU(\phi)\rho_tU^\dagger(\phi) + U(\phi)\rho_t\partial_kU^\dagger(\phi),\end{aligned}\tag{C.1}$$

where $U(\phi) = e^{-itH(\phi)}$. Detailed calculation [68]:

$$\begin{aligned}\partial_kU(\phi) &= \partial_k e^{-itH(\phi)} \\ &= -i \int_0^t du e^{-i(t-u)H(\phi)} [\partial_k H(\phi)] e^{-iuH(\phi)} \\ &= -i e^{-itH(\phi)} \int_0^t du e^{iuH(\phi)} J_k e^{-iuH(\phi)} \\ &= -iU(\phi)A_k,\end{aligned}\tag{C.2}$$

where

$$A_k = \int_0^t du e^{iuH(\phi)} J_k e^{-iuH(\phi)},\tag{C.3}$$

is a Hermitian operator [38, 68, 69]. To solve Eq. (C.3), we follow the method described in Refs. [68, 69], and we use this form to calculate QFIM. Therein, for $t \ll 1$, we have

$$A_k \approx tJ_k.\tag{C.4}$$

For arbitrary large t , we have [68, 69]

$$A_k = t \sum_{\{l|\lambda_l=0\}} \text{Tr}[\Gamma_l^\dagger J_k] \Gamma_l - i \sum_{\{l|\lambda_l \neq 0\}} \frac{1 - e^{-i\lambda_l t}}{\lambda_l} \text{Tr}[\Gamma_l^\dagger J_k] \Gamma_l,\tag{C.5}$$

where Γ satisfies the eigenvalue equation:

$$\mathcal{H}(\phi)\Gamma \equiv [H(\phi), \Gamma] = \lambda\Gamma.\tag{C.6}$$

$\mathcal{H}(\phi)$ is a Hermitian superoperator of $H(\phi)$, which has d_D^2 real eigenvalues: $\lambda_1, \dots, \lambda_{d_D^2}$. We also denote $\Gamma_l, l = 1, \dots, d_D^2$ are orthonormal eigenvalues of Γ .

Finally, substituting Eq. (C.1) into Eq. (7) in the main text, we obtain the QFIM.

-
- | | |
|---|---|
| <p>[1] L. Pezzé and A. Smerzi, Phys. Rev. Lett. 102, 100401 (2009).</p> <p>[2] S. F. Huelga, C. Macchiavello, T. Pellizzari, A. K. Ekert, M. B. Plenio, and J. I. Cirac, Phys. Rev. Lett. 79, 3865 (1997).</p> <p>[3] D. J. Wineland, J. J. Bollinger, W. M. Itano, F. L. Moore, and D. J. Heinzen, Phys. Rev. A 46, R6797 (1992).</p> <p>[4] D. J. Wineland, J. J. Bollinger, W. M. Itano, and D. J. Heinzen, Phys. Rev. A 50, 67 (1994).</p> <p>[5] V. Giovannetti, S. Lloyd, and L. Maccone, Science 306, 1330 (2004), https://science.sciencemag.org/content/306/5700/1330.full.pdf.</p> <p>[6] V. Giovannetti, S. Lloyd, and L. Maccone, Phys. Rev. Lett. 96, 010401 (2006).</p> | <p>[7] J. A. Jones, S. D. Karlen, J. Fitzsimons, A. Ardavan, S. C. Benjamin, G. A. D. Briggs, and J. J. L. Morton, Science 324, 1166 (2009), https://science.sciencemag.org/content/324/5931/1166.full.pdf.</p> <p>[8] S. Simmons, J. A. Jones, S. D. Karlen, A. Ardavan, and J. J. L. Morton, Phys. Rev. A 82, 022330 (2010).</p> <p>[9] S. Zaiser, T. Rendler, I. Jakobi, T. Wolf, S.-Y. Lee, S. Wagner, V. Bergholm, T. Schulte-Herbrüggen, P. Neumann, and J. Wrachtrup, Nature Communications 7, 12279 (2016).</p> <p>[10] Y. Matsuzaki, S. Benjamin, S. Nakayama, S. Saito, and W. J. Munro, Phys. Rev. Lett. 120, 140501 (2018).</p> <p>[11] L. Zhang, A. Datta, and I. A. Walmsley, Phys. Rev. Lett. 114, 210801 (2015).</p> |
|---|---|

- [12] S. Pang, J. Dressel, and T. A. Brun, *Phys. Rev. Lett.* **113**, 030401 (2014).
- [13] S. Pang and T. A. Brun, *Phys. Rev. A* **92**, 012120 (2015).
- [14] S. Pang and T. A. Brun, *Phys. Rev. Lett.* **115**, 120401 (2015).
- [15] A. N. Jordan, J. Tollaksen, J. E. Troupe, J. Dressel, and Y. Aharonov, *Quantum Studies: Mathematics and Foundations* **2**, 5 (2015).
- [16] L. B. Ho and Y. Kondo, *Physics Letters A* **383**, 153 (2019).
- [17] S. Zhou, M. Zhang, J. Preskill, and L. Jiang, *Nature Communications* **9**, 78 (2018).
- [18] Y. Matsuzaki, S. C. Benjamin, and J. Fitzsimons, *Phys. Rev. A* **84**, 012103 (2011).
- [19] W. Dür, M. Skotiniotis, F. Fröwis, and B. Kraus, *Phys. Rev. Lett.* **112**, 080801 (2014).
- [20] D. A. Herrera-Martí, T. Gefen, D. Aharonov, N. Katz, and A. Retzker, *Phys. Rev. Lett.* **115**, 200501 (2015).
- [21] G. Arrad, Y. Vinkler, D. Aharonov, and A. Retzker, *Phys. Rev. Lett.* **112**, 150801 (2014).
- [22] E. M. Kessler, I. Lovchinsky, A. O. Sushkov, and M. D. Lukin, *Phys. Rev. Lett.* **112**, 150802 (2014).
- [23] Y. Matsuzaki and S. Benjamin, *Physical Review A* **95**, 032303 (2017).
- [24] R. Demkowicz-Dobrzański, J. Czajkowski, and P. Sekatski, *Phys. Rev. X* **7**, 041009 (2017).
- [25] J. M. Taylor, P. Cappellaro, L. Childress, L. Jiang, D. Budker, P. R. Hemmer, A. Yacoby, R. Walsworth, and M. D. Lukin, *Nature Physics* **4**, 810 (2008).
- [26] G. de Lange, D. Ristè, V. V. Dobrovitski, and R. Hanson, *Phys. Rev. Lett.* **106**, 080802 (2011).
- [27] L. Cohen, Y. Pilnyak, D. Istrati, A. Retzker, and H. S. Eisenberg, *Phys. Rev. A* **94**, 012324 (2016).
- [28] T. Unden, P. Balasubramanian, D. Louzon, Y. Vinkler, M. B. Plenio, M. Markham, D. Twitchen, A. Stacey, I. Lovchinsky, A. O. Sushkov, M. D. Lukin, A. Retzker, B. Naydenov, L. P. McGuinness, and F. Jelezko, *Phys. Rev. Lett.* **116**, 230502 (2016).
- [29] L. B. Ho, Y. Matsuzaki, M. Matsuzaki, and Y. Kondo, *New Journal of Physics* **21**, 093008 (2019).
- [30] L. B. Ho, Y. Matsuzaki, M. Matsuzaki, and Y. Kondo, “Nuclear magnetic resonance model of an entangled sensor under noise,” (2019), arXiv:1910.13599 [quant-ph].
- [31] A. W. Chin, S. F. Huelga, and M. B. Plenio, *Physical review letters* **109**, 233601 (2012).
- [32] K. Macieszczak, *Physical Review A* **92**, 010102 (2015).
- [33] T. Tanaka, P. Knott, Y. Matsuzaki, S. Dooley, H. Yamaguchi, W. J. Munro, and S. Saito, *Physical review letters* **115**, 170801 (2015).
- [34] A. Smirne, J. Kołodyński, S. F. Huelga, and R. Demkowicz-Dobrzański, *Physical review letters* **116**, 120801 (2016).
- [35] J. F. Haase, A. Smirne, J. Kołodyński, R. Demkowicz-Dobrzański, and S. F. Huelga, *New Journal of Physics* **20**, 053009 (2018).
- [36] S. Dooley, E. Yukawa, Y. Matsuzaki, G. C. Knee, W. J. Munro, and K. Nemoto, *New Journal of Physics* **18**, 053011 (2016).
- [37] F. Albarelli, J. F. Friel, and A. Datta, *Phys. Rev. Lett.* **123**, 200503 (2019).
- [38] T. Baumgratz and A. Datta, *Phys. Rev. Lett.* **116**, 030801 (2016).
- [39] M. D. Vidrighin, G. Donati, M. G. Genoni, X.-M. Jin, W. S. Kolthammer, M. S. Kim, A. Datta, M. Barbieri, and I. A. Walmsley, *Nature Communications* **5**, 3532 (2014).
- [40] M. Altorio, M. G. Genoni, M. D. Vidrighin, F. Somma, and M. Barbieri, *Phys. Rev. A* **92**, 032114 (2015).
- [41] M. Szczykulska, T. Baumgratz, and A. Datta, *Quantum Science and Technology* **2**, 044004 (2017).
- [42] S. I. Knysh and G. A. Durkin, “Estimation of phase and diffusion: Combining quantum statistics and classical noise,” (2013), arXiv:1307.0470 [quant-ph].
- [43] P. J. D. Crowley, A. Datta, M. Barbieri, and I. A. Walmsley, *Phys. Rev. A* **89**, 023845 (2014).
- [44] O. Pinel, P. Jian, N. Treps, C. Fabre, and D. Braun, *Phys. Rev. A* **88**, 040102 (2013).
- [45] C. N. Gagatsos, B. A. Bash, S. Guha, and A. Datta, *Phys. Rev. A* **96**, 062306 (2017).
- [46] E. Roccia, V. Cimini, M. Sbroscia, I. Gianani, L. Ruggerio, L. Mancino, M. G. Genoni, M. A. Ricci, and M. Barbieri, *Optica* **5**, 1171 (2018).
- [47] M. G. Genoni, M. G. A. Paris, G. Adesso, H. Nha, P. L. Knight, and M. S. Kim, *Phys. Rev. A* **87**, 012107 (2013).
- [48] S. Steinlechner, J. Bauchrowitz, M. Meinders, H. Müller-Ebhardt, K. Danzmann, and R. Schnabel, *Nature Photonics* **7**, 626 (2013).
- [49] V. Cyril, T. Tommaso, and G. M. G., “qmetro,” (2013) Chap. Quantum estimation of a two-phase spin rotation, p. 12.
- [50] P. C. Humphreys, M. Barbieri, A. Datta, and I. A. Walmsley, *Phys. Rev. Lett.* **111**, 070403 (2013).
- [51] N. Liu and H. Cable, *Quantum Science and Technology* **2**, 025008 (2017).
- [52] A. Monras and F. Illuminati, *Phys. Rev. A* **83**, 012315 (2011).
- [53] D. W. Berry, M. Tsang, M. J. W. Hall, and H. M. Wiseman, *Phys. Rev. X* **5**, 031018 (2015).
- [54] A. Fujiwara, *Phys. Rev. A* **65**, 012316 (2001).
- [55] M. A. Ballester, *Phys. Rev. A* **69**, 022303 (2004).
- [56] D. Le Sage, K. Arai, D. R. Glenn, S. J. DeVience, L. M. Pham, L. Rahn-Lee, M. D. Lukin, A. Yacoby, A. Komeili, and R. L. Walsworth, *Nature* **496**, 486 (2013).
- [57] A. Nowodzinski, M. Chipaux, L. Toraille, V. Jacques, J.-F. Roch, and T. Debuisschert, *Microelectronics Reliability* **55**, 1549 (2015).
- [58] A. Shankar, J. Cooper, J. G. Bohnet, J. J. Bollinger, and M. Holland, *Physical Review A* **95**, 033423 (2017).
- [59] P. Kirton and J. Keeling, *Physical review letters* **118**, 123602 (2017).
- [60] N. Shammah, S. Ahmed, N. Lambert, S. De Liberato, and F. Nori, *Phys. Rev. A* **98**, 063815 (2018).
- [61] D. Chruściński and S. Pascazio, *Open Systems & Information Dynamics* **24**, 1740001 (2017), <https://doi.org/10.1142/S1230161217400017>.
- [62] K. HUSIMI, *Proceedings of the Physico-Mathematical Society of Japan*.
- [63] W. Gorecki, S. Zhou, L. Jiang, and R. Demkowicz-Dobrzański, “Optimal probes and error-correction schemes in multi-parameter quantum metrology,” (2019), arXiv:1901.00896 [quant-ph].
- [64] B. A. Chase and J. M. Geremia, *Phys. Rev. A* **78**, 052101 (2008).
- [65] B. Q. Baragiola, B. A. Chase, and J. Geremia, *Phys. Rev. A* **81**, 032104 (2010).
- [66] V. V. Mihailov, *Journal of Physics A: Mathematical and General* **10**,
- [67] R. H. Dicke, *Phys. Rev.* **93**, 99 (1954).

- [68] R. M. Wilcox, Journal of Mathematical Physics **8**, 962 (1967)[69] S. Pang and T. A. Brun, Phys. Rev. A **90**, 022117 (2014).
<https://doi.org/10.1063/1.1705306>.